Indian Journal of Ecology (2022) 49 Special Issue (18): 675-683

Manuscript Number: S-891
NAAS Rating: 5.79

Synthesis and Characterization of Spinal Ferrite MFe_2O_4 (M = Co/Zn) Nanoparticles for Lead (II) Ions Removal from Aqueous Solution

Ahmed Y. Hammo, Tarik E. Jassim` and Mohanad J.K. AL. Asadi`

Department of Marine Environmental Chemistry, Marine Science Center
`Department of Chemistry, College of Education for Pure Science, University of Basrah, Basrah, Iraq
E-mail: ahmed_yh79@yahoo.com

Abstract: Ferrite nanoparticles (NPs) with structure MFe_2O_4 (M = Co/Zn) were created flowing the sol-gel auto-combustion technique using lemon juice as surfactant and fuel agent. Nanomaterials were diagnosed using different physical and chemical techniques. The susceptibility of the produced nanomaterials as adsorbents of lead ions was examined. The nanoparticles synthesis in this study has structural and chemical characteristics that have been described using different technologies: Brunauer–Emmett–Teller (BET) analysis, Field emission-scanning electron microscopy (FE-SEM), Energy Dispersive X-ray Spectroscopy (EDX), Fourier-transform infrared spectroscopy (FTIR), transmission electron microscopy (TEM) and X-ray diffraction (XRD). Synthesized ferrite NPs were analyzed as removal agent for lead ions. The effects of adsorbent concentration, pH, temperature and time of contact on lead ion uptake behavior were measured. The results showed that adsorption has strong correlation with Freundlich model compared with the Langmuir model. The thermodynamic parameters revealed endothermic reaction for ΔH, ΔG was found aspontaneous process and ΔS were found positive value.

Keywords: Adsorption, Pb(II) ions, ferrite nanoparticles, Langmuir, Frendlich, Thermodynamic

Water shortage, both of quantity and quality, has be the main threat to humanity's well-being. With the speedy escalation of industrialization, the drinking water quality has become a worrisome topic. Contamination is primarily caused by waste products produced by the textile, chemical, mining, and metallurgical industries (Agustin et al 2011). Water usually polluted with different heavy metal ions like (As, Zn, Co, Ni, Hg, Cd, Pb, and Cr) in addition to other pollutants with organic origin (Shen et al 2009). One of the modern issues is contamination water by dangerous metal particles like Cd(II), Pb(II) and pollution by a microorganism. Many materials are used to remove heavy metals especially if they are able to absorb the ions but depend on the efficiency and performance of the process. The established many approaches to channel the waste water such precipitation, particle trade, buoyancy, oxidation electrochemical medications, adsorption, invert osmosis, dissipation, film filtration, and biosorption procedures are broadly utilized (Chen et al 2009, Ivanov et al 2004). Improvement of the novel and financially savvy nanomaterials for natural remediation, contamination discovery and different applications are in extensive consideration. Late advances propose that a number of problems including quality of water can be settled or it has been developed using different nanotechnologies such as nanoparticles and nanofiltration in addition to the other tools resulting from the progress of this technology(Jurgen and Joydeep 2005, Salman et al 2017).

Spinel ferrites have recently identified as a new class of adsorbents that are preferably for water treatment (Kefeni et al 2017,Chinh et al 2020). It is suitable for removing impurities because it has large surface area and many effective sites. Spinel ferrites can be removed from reaction mixture effortlessly using an external magnetic field as they have superior superparamagnetic properties (SPM) (Baig and Varma 2013, Nasir et al 2015). Spinel ferrites have been studied for their ability to remove organic compounds, nutrient salts, and toxic metals from water (Roonasi and Nezhad 2016). Usually the universal formula of spinel ferrites is MFe_2O_4 (where M: Fe, Co, Ni, Zn, etc.) and cubic structure consists of 32 O- atoms which occupied by 8 Td (tetra-herbal) and 16 Oh (octahedral) occupied sites. When magnetic spinel ferrites are prepared as nanoparticles, the smaller particle size and high surface area reinforce its capacity for as removal (Cafer et al 2006).

Many synthetic procedures were utilized to prepare the magnetic highly crystalline and uniformly sized nanoparticles of cobalt-ferrites and zinc- ferrites by precipitation method. the coprecipitation method (Mahboubeh et al 2014, Baykal et al 2012), the hydrothermal method (Zhao et al 2007), the sol-gel method (Sivakumar et al 2012) and the sol-gel auto-

combustion method (Ismat et al 2017). In current work, $CoFe_2O_4$ and $ZnFe_2O_4$, ferrite sample was created by the sol-gel auto-combustion technique, using lemon juice as surfactant and fuel factor. This technology is considered environmentally friendly and cost effective as against the conventional synthesis of technologies.

MATERIAL AND METHODS

Synthesis of MFe_2O_4 (M = Co/Zn) nanoparticles: The process for synthesis of $CoFe_2O_4$ and $ZnFe_2O_4$ was carried out as follow:

1- 14.54g of $Fe(NO_3)_3.9H_2O$ (M.W 404) was mixed with 10.4g of $Co(NO_3)_2.6H_2O$ (M.W 290.93), 9.4g of Zn $(NO_3)_2.6H_2O$ (M.W 290.69) and dissolved in 45ml of lemon juice extract.
2- Ammonia solution (NH_4OH) was added in order to keep the pH of the solution to 7.0 with continuous stirring using a magnetic stirrer.
3- Continuous for stirring half an hour at 80°C, the clear sol. was completely turned to a gel.
4- Oven desiccates at 80°C to get a steady weighing and grinded to fine powder, then calcined at 600°C for 5 hours in furnace under air atmosphere.

Characterization techniques: For the purpose of diagnosis, many advanced and highly efficient technologies are used worldwide have been used. These are represented by X-ray diffraction (XRD), transmission electron microscopy (TEM), Brunauer–Emmett–Teller (BET) surface area study, scanning electron microscopy with energy dispersive X-ray spectroscopy (FESEM -EDX). For calculation of the Pb(II) the flame atomic absorption spectrophotometer (AAS) has been used.

Adsorption studies: The stock solution of lead was prepared by melting 1.59 g of lead nitrate Pb $(NO_3)_2$ in 1000 ml of distilled deionized water and from this concentration several other dilute solutions were prepared. To determine the ideal pH, both NaOH (0.1 M) and HCL (0.1 M) were used to obtain the pH range (3-9). Perfect contact time (5-180 min) for adsorption of Pb(II) was determined using batch method ,where 0.05 g adsorbent was added to 25 ml solution with concentration (100 mg l^{-1}) putted in 100 ml flasks. Different temperature (10.0, 25.0, 37.5 and 50.0°C), was used for equilibration, with agitation rate 120 rpm using an orbital shaker. The amount of ions adsorbed and removal percent of adsorbent was calculated as differ between the concentration of the ion before and after adsorption from relation (Palak et al 2019).

$$Qe = V(C_0 - C_e)/m \quad .....(1)$$

$$Removal(\%) = [(C_0 - C_e)/C_0] \times 10 \ldots\ldots(2)$$

Where; Q_e the capacity of adsorption at equilibrium (mg g^{-1}), V represent the volume (l) of solution , m is the adsorbent weight (g),Co = the primary concentration of solution in mg l^{-1}, Ce = concentration of solution after adsorbent. Equation Langmuir and Freundlich used for data analysis.

Thermodynamic parameters: From stock solution of Pb(II) different concentration with range (60-120) mg l^{-1} was prepared, putted in the flask and subsequently add 0.05g $CoFe_2O_4$ and $ZnFe_2O_4$ to every concentration. The flask was exposed to shake at 120 rpm and in the right balance time at different temperatures (10.0, 25.0, 37.5 and 50.0°C). Centrifuge the mixture and determine the lead ion concentration. ΔG is the variations in free energy; enthalpy ΔH and entropy ΔS related to the adsorption process were calculation as follow:

$$\Delta G = -RT \ln k \ldots..(3)$$

$$K = C_{solid} / C_{liquid} \ldots\ldots(4)$$

$$\ln K = \Delta S / R - \Delta H / RT \ldots..(5)$$

Where ΔG is the change of Gibbs energy change (KJ mol^{-1}), K is the constant of equilibrium, C_{solid} is the concentration at equilibrium for the solid phase concentration (mg L^{-1}), C_{liquid} is the concentration at equilibrium for the liquid phase (mg L^{-1}), T is the temperature in Kelvin and R is constant of the gas (0.0083 KJ $K^{-1}mol^{-1}$). ΔH (KJ mol^{-1}) and ΔS (KJ mol^{-1} k^{-1}) can be calculated from the slope and intercept of Eq.(5)(Huacai and Ziwei 2015).

RESULTS AND DISCUSSION

FT-IR spectroscopy: The FTIR spectra of the samples were calcified at 100°C (Fig. 1a,b). The infrared spectrum recorded many absorption peaks at the range 4000 cm^{-1} to 400 cm^{-1}. The peak observed at 3431.36 cm^{-1} for $CoFe_2O_4$, 3437.15 cm^{-1} for $ZnFe_2O_4$. It is attributed to the stretching vibrations of the of hydroxide(0-H) bond. The band at 1616.35cm^1 is attributable to H–O–H bending vibration mod, which indicates the adsorption of water on ferrite (Anandan and Rajendran 2011). Furthermore, the nitrate group showed a stretching vibration in the wave 1388 cm^1, in the prepared samples the nitrate ions were present (Ghasemi 2015) . The position of spinel ferrite finds in the region of 400–600 cm-1 by (Co-O), (Zn-O) and (Fe-O) stretching vibration (Shaima'a and Ali 2018).

X-ray diffraction (XRD): The identification output for the prepared sample (CoFe2O4 and ZnFe2O4) by X-ray diffraction (XRD) given in Figure 2 (A and B). The output displays perfect crystallization properties and single phase. The standard data (JCPDS No. 22-1086 for $CoFe_2O_4$ and JCPDS No. 22-1012 (Paveena et al 2011, Jiang and Ai 2010) for $ZnFe_2O_4$ has been used for comparison with the present results, and the comparison results proved that both of the two study samples can be included within the spinel cubic

designated in the reflecting planes (111), (220), (311), (400), (422), (511),(440) and (533) in the patterns, The crystallite sizes were calculated using XRD peak broadening of the (311) peak using the Scherer's formula:

$\tau_{hkl=}(K*\lambda)/(\beta_{hkl}*\cos(\theta_{hkl})$ **..... (6)**

Where τ is the particle size perpendicular to the normal line of (hkl) plane, β_{hkl} is the full width at half maximum, θ_{hkl} is the Bragg angle of (hkl) peak, K is constant equal 0.9 and λ is the wavelength of X-ray. The particle size of nanoparticles calculated at 600°C is about 56.68nm for $CoFe_2O_4$ and 21.22nm for $ZnFe_2O_4$.

Surface morphology and elemental analysis: Field Emission Scanning Electron Microscopy (FESEM) analysis was used to investigate the morphology of as-prepared bare $CoFe_2O_4$ and $ZnFe_2O_4$ nanoparticles. Figure 3(A and B) shows that the bare $CoFe_2O_4$ and $ZnFe_2O_4$ particles were quasi-spherical with small agglomeration. On the other hand, Figure 4 (A and B) presents the TEM images $CoFe_2O_4$ and $ZnFe_2O_4$ nanoparticles. The image showed the presence of pores and voids within a network formed as a result of the deposition of gases through the reaction of combustion. This is typical of combustion-synthesized powders. The samples the particles are roughly spherical. Compositional purity was confirmed by analysis (EDX) various regions of each sample can be examined. In addition the use of EDX technology offers many possibilities in terms of sample components and elements' mapping. The Figure 5 (A and B) shows the EDX spectra of the prepared $CoFe_2O_4$ and $ZnFe_2O_4$. Through the results, it is clear that the elements Co, Zn, O, and Fe were present in different proportions without the presence of any impurities.

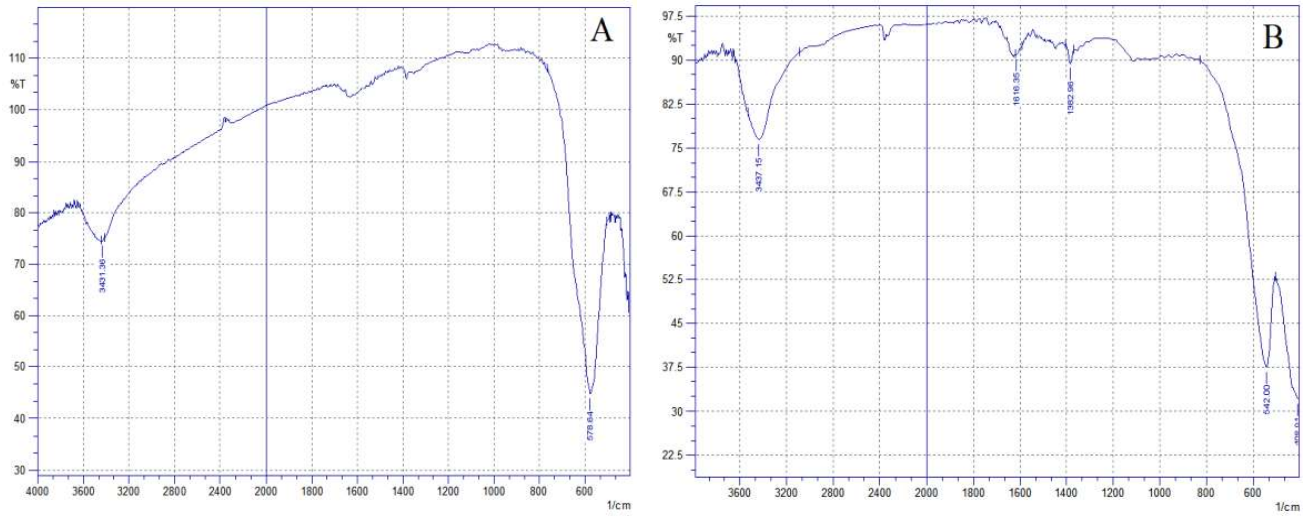

Fig. 1. FT-IR spectra (A) $CoFe_2O_4$ (B) $ZnFe_2O_4$

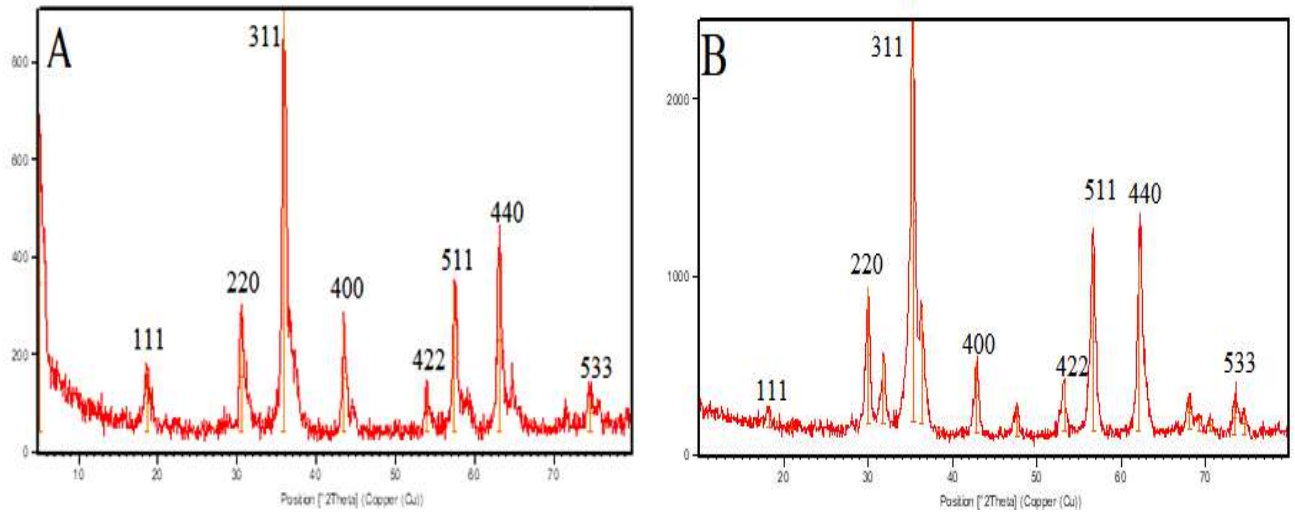

Fig. 2. Phase identification of a crystalline patterns synthesis nanoparticles of (A) $CoFe_2O_4$ (B) $ZnFe_2O_4$

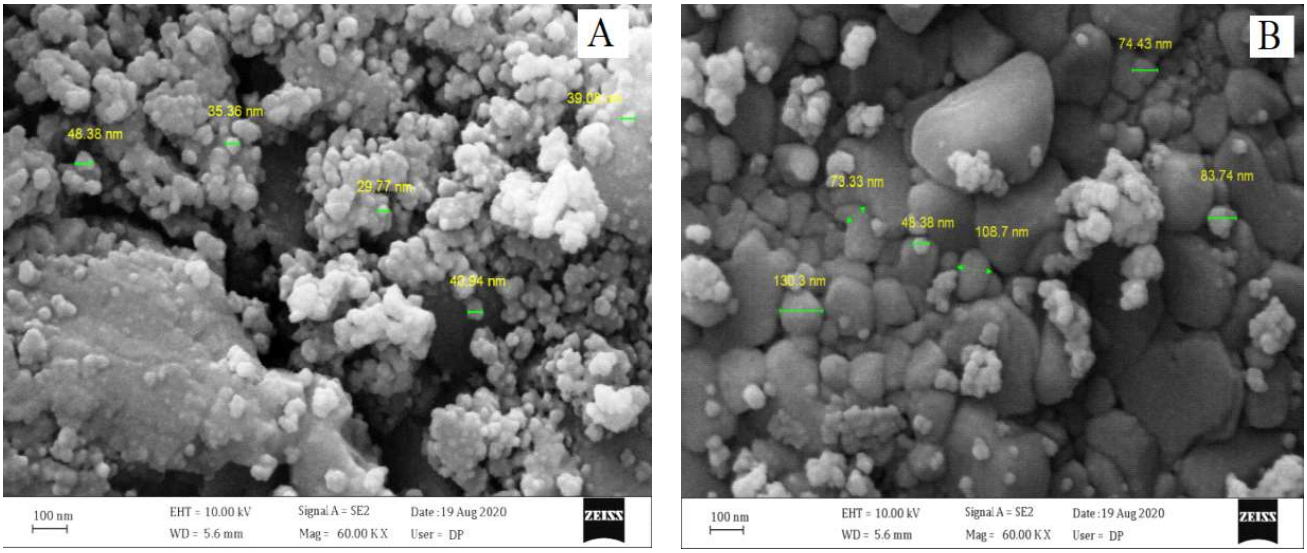

Fig. 3. FESEM photographesof (A) $CoFe_2O_4$ (B) $ZnFe_2O_4$

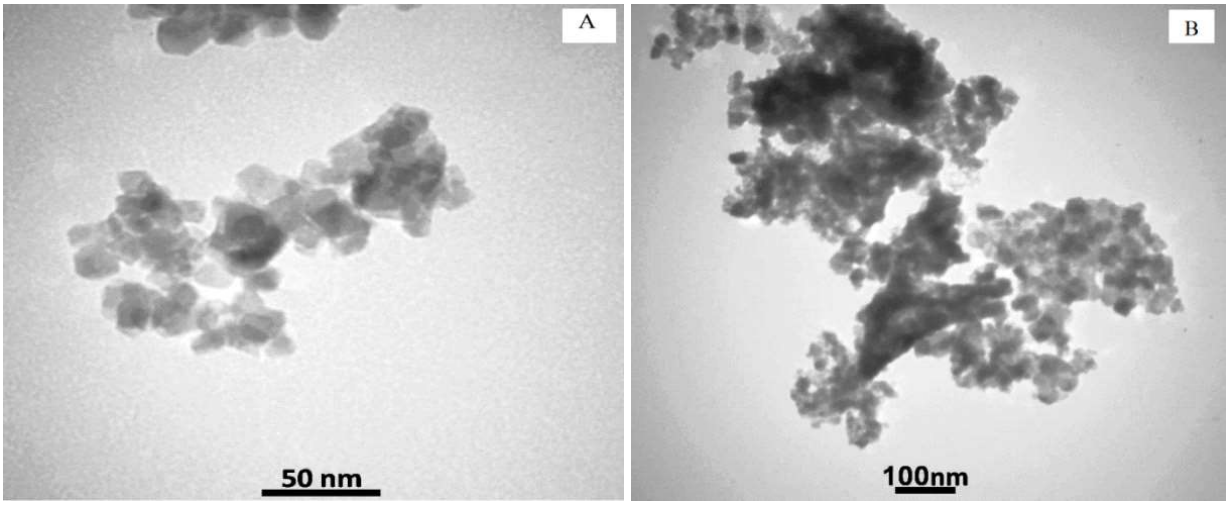

Fig. 4. Transsmision electron micrograph of (A) $CoFe_2O_4$ (B) $ZnFe_2O_4$

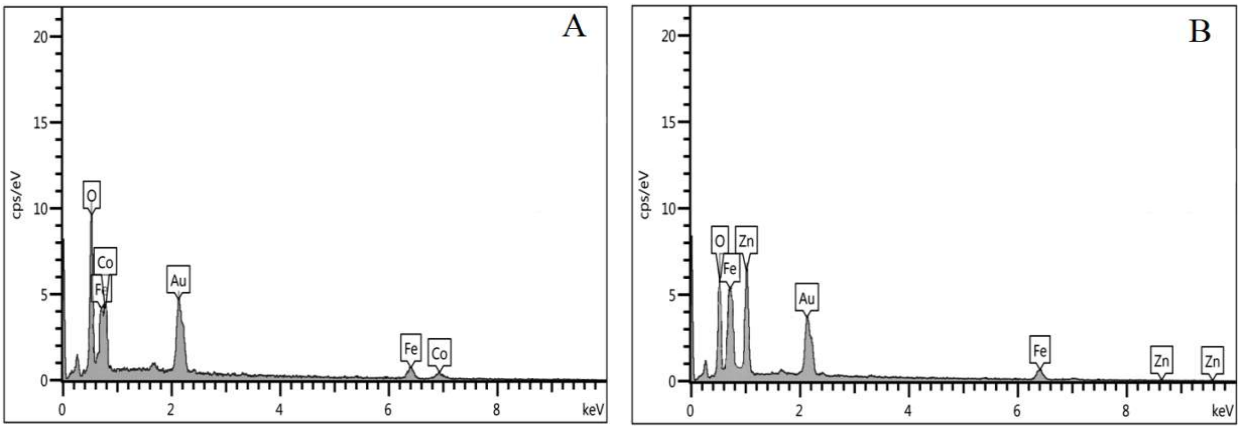

Fig. 5. EDX spectra of (A) $CoFe_2O_4$ (B) $ZnFe_2O_4$

Brunauer–Emmett–Teller (BET): The nitrogen adsorption–desorption isotherms of $CoFe_2O_4$ and $ZnFe_2O_4$ NPs was observed using Brunauer–Emmett–Teller (BET) analysis (Fig. 6 A and B). The BET surface area for $CoFe_2O_4$ and $ZnFe_2O_4$ NPs was 8.755 and 1115.3 $m^2 g^{-1}$, respectively. The higher surface area of $ZnFe_2O_4$ nanoparticles could credit to the reduction in the size of grain. Figure 6 (A and B) also shows the pore size allocation of the produced nanoparticles. The $CoFe_2O_4$ and $ZnFe_2O_4$ have average mean pore diameters 7.99 and 1.21 nm, respectively which is due to pores form between grains of metal oxides.

Adsorption Studies

Effect of contact time: Different period of time (5-180 min) at fixed temperature (25°C) was used to investigate the influence of contact time on the Pb (II) ion adsorption. Figure 7 (A and B) shows increase in the removal percentages of Pb (II) ions by increasing the period of contacting till reaching to the equilibrium. The adsorption amount was high in the beginning because there is a large adsorption surface area suitable for the attaching the Pb (II) ions. At the end the adsorption rate is slower probably due to active sites become saturation and equilibrium is stabilized (El-Ashtoukhy et al 2008, Pehlivan et al 2009). The equilibrium time was 60min for $CoFe_2O_4$ and 15min for $ZnFe_2O_4$. The percentage of Pb (II) ions removal in $CoFe_2O_4$ and $ZnFe_2O_4$ nanoparticles were 62.05 and 95.74% respectively.

Effect of pH on the adsorption: Acidity is a significant aspect that affects the metal adsorption in the aqueous solution during solid–water interfaces. The accessibility of metal ions in the solution and the binding sites of the adsorbent are affected by pH. The influence of the pH on the adsorption of Pb(II) ions on $CoFe_2O_4$ and $ZnFe_2O_4$ nanoparticles in various pH (pH=3, 5, 7 and 9) was studied by using affixed concentration 100 mg/l and time of (60, 15min) for $CoFe_2O_4$ and $ZnFe_2O_4$ respectively of 25°C. The Fig. 8A and B, prove the effect of pH on the adsorption.

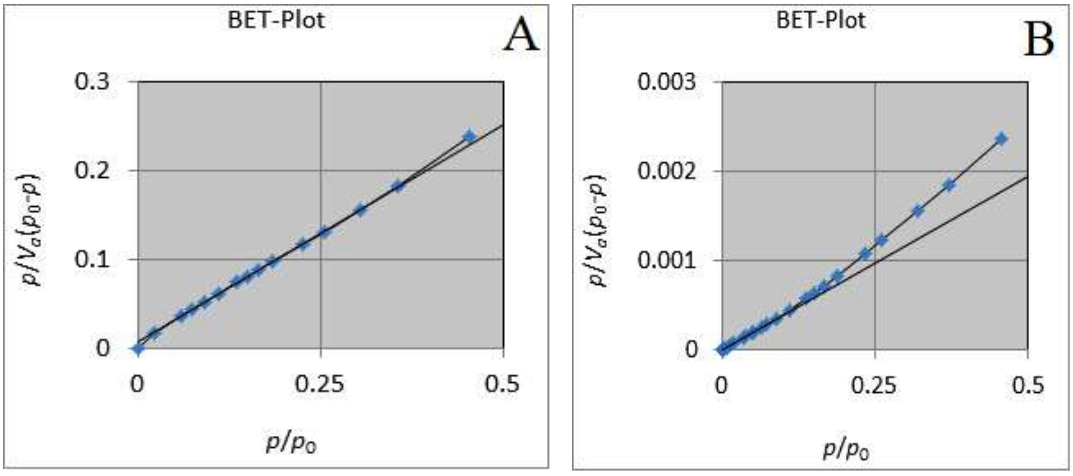

Fig. 6. BET of (A) $CoFe_2O_4$ and (B) $ZnFe_2O_4$

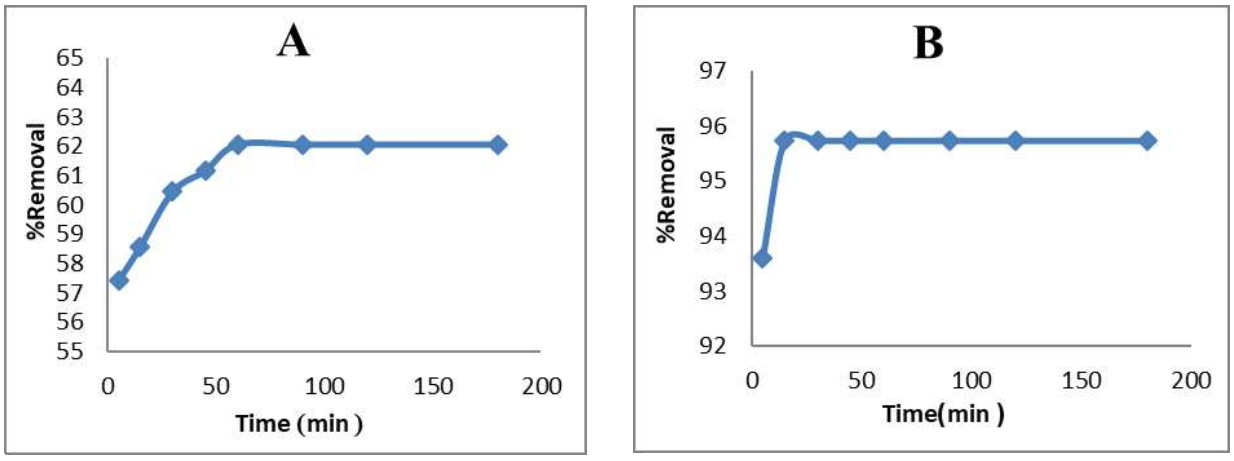

Fig. 7. Effect of contact time of (A) $CoFe_2O_4$ and (B) $ZnFe_2O_4$

The removal of Pb (II) percentage was toward the basal (Fig. 8). The active sites gain a positive charge in the presence of an acidic medium (low pH) with the presence of hydronium ions, leading to the repulsion between the positive charge metals and the adsorbent. Binding sites begin to deprotonate at higher pH values, making various functional groups accessible for binding the metal. In general, cation binding increases as pH rises; however, as pH rises, the solubility of Pb(II) ions decreases, resulting in an increase in the adsorption affinity towards the surfaces of $CoFe_2O_4$ and $ZnFe_2O_4$ (Esposito et al 2002). Accordingly, the pH of 5 was chosen to carry out the experiment to avoid uncertain results, as other mechanisms such as sedimentation play a role in removing the metals.

Adsorption isotherm: Various temperatures (10, 25, 37.5, 50°C), were chosen to exam the ability of $CoFe_2O_4$ and $ZnFe_2O_4$ nanoparticles to remove Pb (II) from aqueous solution. Figure 9 (A and B) shows the isotherm adsorption of Pb (II), where the amounts adsorbed on $CoFe_2O_4$ and $ZnFe_2O_4$ (Qe) planned as a occupation of balance concentricity (Ce).

The Pb (II) ion adsorption isotherm form on the $CoFe_2O_4$ and $ZnFe_2O_4$ nanoparticles consistent with (S-type) in the classification of Giles. S-Curve , revealed vertical or flat alignment of adsorbate . There is a strong inter-molecular attraction within the adsorbed layer, the more solute is already adsorbed, and the easier it is for additional amounts to become fixed (Giles et al 1960). Both of Langmuir isotherm and Freundlich equation were used to apply the experimental adsorption results. The effects by using Freundlich's (eq. 7) and Langmuir's (eq. 8) equations (Veena and Robert 2002). Table 1 shows the adsorbents isotherm data .

$$\log Qe = \log Kf + 1/n \log Ce \quad \ldots\ldots\ldots (7)$$

Where Kf is afanction of the adsorption capacity and n is the intensity of adsorption .

$$Ce/Qe = 1/Qmb + Ce/Qm \quad \ldots\ldots\ldots (8)$$

Where Q_m is the maximum sorption capacities (mg g^{-1}) and b is related to the sorption energy.

The Freundlich and Langmuir isotherms are applied on the empirical data of the adsorption of Pb(II) ions on CoFe2O4 and ZnFe2O4 nanoparticles by plotting log Qe versus log Ce and Ce /Qe versus Ce respectively (Fig. 10 and

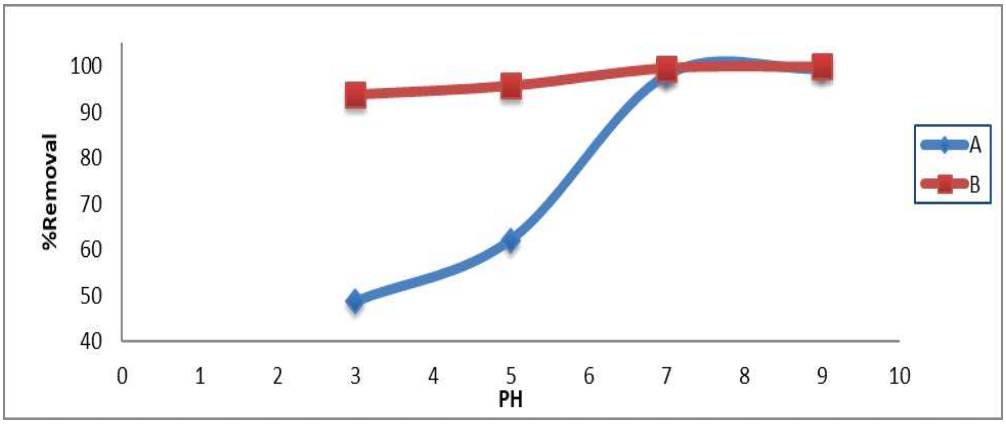

Fig. 8. Effect of pH on Pb(II) adsorption of (A) $CoFe_2O_4$ and (B) $ZnFe_2O_4$

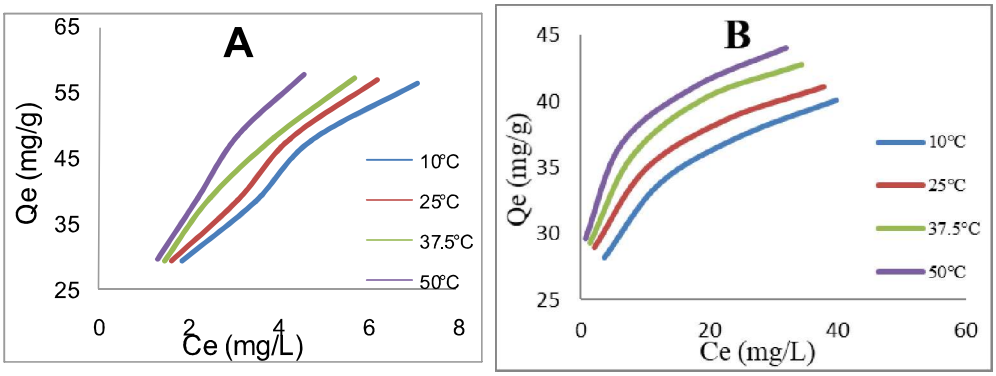

Fig. 9. Adsorption isotherm of Pb(II) on (A) $CoFe_2O_4$ and (B) $ZnFe_2O_4$ nanoparticles at various temperatures

11). The R^2 values for the Freundlich model are closer to unity than Langmuir for adsorption process onto $CoFe_2O_4$ and $ZnFe_2O_4$ (Table 1). This proves that the application of the Freundlich model was better in characterizing the Pb (II) ions adsorption on $CoFe_2O_4$ and $ZnFe_2O_4$ nanoparticles than the Langmuir models and it is the most accurate characterization of the multi-layer adsorption method on the surface of a heterogeneous adsorbent surface.

Thermodynamics: The effect of temperature on Pb(II)ion adsorption was investigated using different initial concentrations and temperatures ranging from (10 - 50C°). The parameters of thermodynamic are represented by (ΔG), (ΔH), and (ΔS) was used to assessment the feasibility the adsorption method (Table 2). The relationship was linear between lnK against1/T with a correlation coefficient (R^2 = 0.944 – 0.975) and (0.916 – 0.996) for Pb (II) ion adsorption

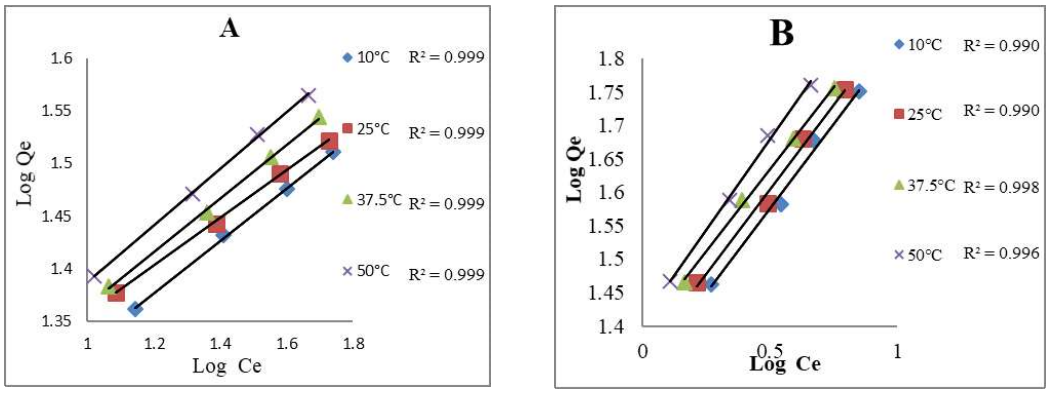

Fig. 10. The Freundlich isotherms linear form of Pb(II) on (A) $CoFe_2O_4$ and (B) $ZnFe_2O_4$nanoparticles at various temperatures

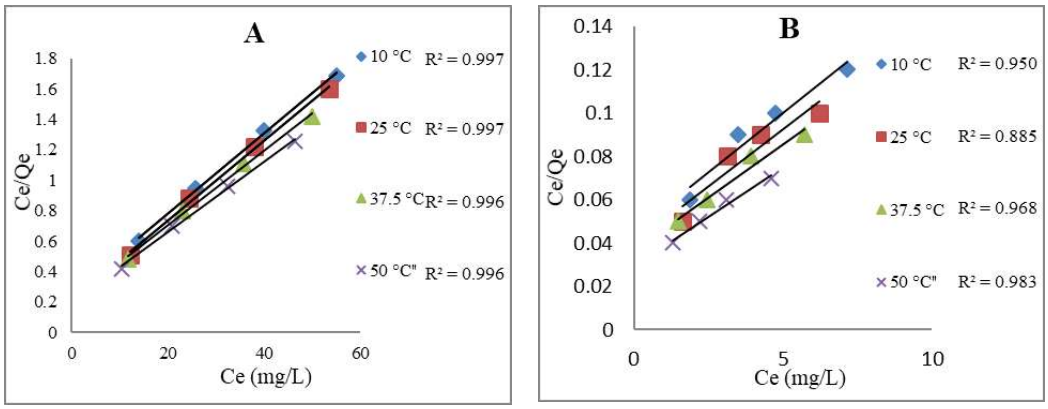

Fig. 11. Langmuir isotherms linear form of Pb(II) on (A) $CoFe_2O_4$ and (B) $ZnFe_2O_4$nanoparticles at various temperatures

Table 1. Isotherm results of the studied system when applying both of Freundlich and Langmuir isotherms

Composition	Temp. (C)	Langmuir constants			Freundlich constants		
		Q_m (mg g^{-1})	b (L mg^{-1})	R^2	n	Kf	R^2
$CoFe_2O_4$	10.0	37.800	0.105	0.997	4.028	12.004	0.999
	25.0	38.093	0.123	0.997	4.410	13.512	0.999
	37.5	40.851	0.113	0.996	3.924	12.886	0.999
	50.0	43.224	0.117	0.996	3.722	13.148	0.999
$ZnFe_2O_4$	10.0	91.182	0.242	0.950	1.978	20.994	0.990
	25.0	95.410	0.261	0.885	1.979	22.482	0.990
	37.5	102.679	0.263	0.968	2.039	24.476	0.998
	50.0	110.144	0.307	0.983	1.846	25.575	0.996

Table 2. Thermodynamic function for absorption both of Pb(II) ions

Composition	Co (mg/L)	K				- ΔG				ΔH	ΔS
		Temperature									
		283	298	310.5	323	283	298	310.5	323		
$CoFe_2O_4$	60	3.307	3.909	4.159	4.719	2.629	3.109	3.509	3.909	6.427	0.032
	80	2.099	2.267	2.476	2.849	1.419	1.794	2.106	2.419	5.656	0.025
	100	1.499	1.635	1.797	2.082	0.683	1.043	1.343	1.643	6.109	0.024
	120	1.178	1.244	1.405	1.580	0.303	0.618	0.880	1.143	5.640	0.021
$ZnFe_2O_4$	60	31.085	35.809	39.816	45.511	7.868	8.663	9.325	9.988	7.131	0.053
	80	21.857	24.641	30.128	39.816	6.934	7.804	8.529	9.254	9.480	0.058
	100	20.052	22.474	24.445	31.154	6.812	7.592	8.242	8.892	7.904	0.052
	120	15.806	18.261	20.015	25.086	6.346	7.126	7.776	8.426	8.370	0.052

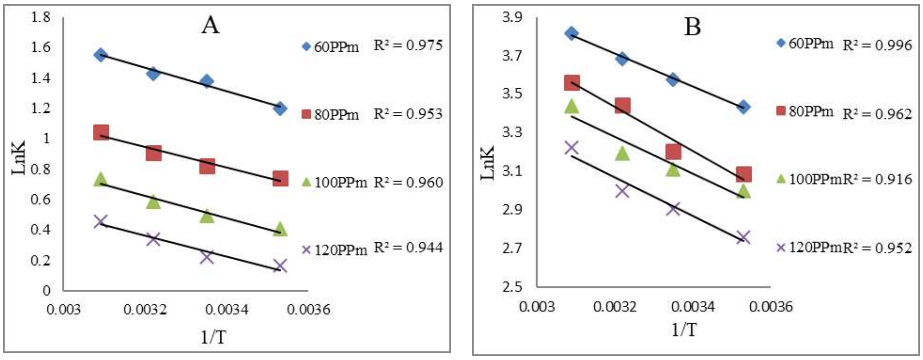

Fig. 12. Plot of LnK against 1/T for adsorption of Pb (II) on (A) $CoFe_2O_4$ and (B) $ZnFe_2O_4$ nanoparticles

on both of CoFe2O4 and ZnFe2O4 nanoparticles (Fig. 12 A and B).

The enthalpy values (ΔH) of adsorption of Pb (II) on (A) $CoFe_2O_4$ and (B) $ZnFe_2O_4$nanoparticles, system possess positive values indicating endothermic adsorption process (Table 2). It is expressed positive value for ΔS through the adsorption process. There was an increase in the randomness of the interference between solid and liquid (Khulood and Sara 2010). The thermodynamic function ΔG value was negative for all temperatures and increased with increasing temperatures, indicating that the adsorption process occurred spontaneously (Hefne et al 2008).

CONCLUSION

In this study, CoFe2O4 and ZnFe2O4nanoparticles ferrites prepared were synthesized by sol-gel auto-combustion process and lemon juice as surfactant and fuel agent. Spinel ferrite with a single-phase was obtained by sample calcination at 600°C, The BET surface area analysis revealed that the as-synthesized materials have a great surface area. The adsorption isotherms were also calculated, and both the Langmuir and Freundlich models accurately represented them, with the Freundlich model fitting better than the Langmuir model. The adsorption reaction was spontaneous and endothermic, according to thermodynamic properties. As a result, the prepared composite may be used as a heavy metal ion adsorbent for environmental applications.

REFERENCES

Agustin G, Jesus LV and Diana MF 2011. Impact of mining activities on sediments in a semi-arid environment: San Pedro River, Sonora, Mexico. *Journal of Applied Geochemistry* **26**: 2101-2112.

Anandan K and Rajendran V 2011. Morphological and size effects of NiO nanoparticles via solvothermal process and their optical properties. *Material. Science in. Semiconductor. Processing* **14**(1): 43-47.

Baig RB and Varma RS 2013. Magnetically retrievable catalysts for organic synthesis. *Chemical Communications* **49**(1): 752-770.

Baykal A, Deligoz H, Sozeri H, Durmus Z and Toprak MS 2012. Triethylene glycol stabilized CoFe2O4 nanoparticles. *Journal of Superconductivity and Novel Magnetism* **25**(1): 1879-1892

Cafer TY, Mayo JT, William W Y, Arjun P, Joshua CF, Sujin Y, Lili C, Heather JS, Amy K, Mason T, Douglas N and Vicki LC 2006. Low-field magnetic separation of monodisperse Fe3O4 nanocrystals. *Science* **314**(1): 964-967.

Chen S, Zou Y, Yan Z, Shen W, Shi S, Zhang X and Wang H 2009. Carboxymethylated bacterial cellulose for copper and lead ion

removal. *Journal of Hazardous Materials* **161**(3): 1355-1359.

Chinh VT, Dang VQ, Hoai PN, Tuan NT and Duong D 2020. Effective Removal of Pb(II) from Aqueous Media by a New Design of Cu-Mg Binary Ferrite. *Journal of American Chemical Society* **5**(2): 7298-7306.

El-Ashtoukhy E, Amina NK and Abdelwahab O 2008. Removal of lead (II) and copper (II) from aqueous solution using pomegranate peel as a new adsorbent. *Journal of Desalination* **223**(1): 162-173.

Esposito A, Pagnanelli F and Veglio F 2002. pH-related equilibria models for biosorption in single metal systems. *Journal of Chemical Engineering Science* **57**(2): 307-313.

Ghasemi A 2015. Compositional dependence of magnetization reversal mechanism, magnetic interaction and Curie temperature of Co1–xSrxFe2O4 spinel thin flm. *Journal of Alloys and Compounds* **645**(1): 467-477.

Giles CH, MamEwans TH, Nakhwa SN and Smith D 1960. Studies in Adsorption. Part XI. A System of Classi$cation of Solution Adsorption Isotherms, and its Use in Diagnosis of Adsorption Mechanisms and in Measurement of Specific Surface Areas of Solids. *Journal of the Chemical Society* **786**(1): 3973-3993.

Hefne JA, Mekhemer WK, Alandis NM, Aldayel OA and Alajyan T 2008. Kinetic and thermodynamic study of the adsorption of Pb(II) from aqueous solution to the natural and treated bentonite. *International Journal of Physical Sciences* **3**(11): 281-288.

Huacai G and Ziwei M 2015. Microwave preparation of triethylenetetramine modifed graphene oxide/chitosan composite for adsorption of Cr(VI*). Journal of Carbohydrate Polymers* **131**(1): 280-287.

Ismat B, Nosheen N, Munawar I, Shagufta K, Haq N, Shazia N, Yursa S, Kashif J, Misbah S, Sadia A, Fariha R and Mazhar A 2017. Green and eco-friendly synthesis of cobalt-oxide nanoparticle: Characterization and photo-catalytic activity. *Journal of Advanced Powder Technology* **28**(1): 2035-2043.

Ivanov V, Tay ST and Jiang HL 2004. Removal of micro-particles by microbial granules used for aerobic wastewater treatment. *Journal of Water Science and Technology* **50**(12): 147-154.

Jiang J and Ai LH 2010. Synthesis and characterization of FeCo binary ferrospinel nanospheres via one-step nonaqueous solution pathway. *Journal of Materials Letters* **64**(8): 945- 947.

Jurgen S and Joydeep D 2005. Nanotechnology in environmental protection and pollution. *Journal of Science and Technology of Advanced Materials* **6**(1): 219-220.

Kefeni KK, Mamba BB and Msagati TA 2017. Application of spinel ferrite nanoparticles in water and wastewater treatment: A review. *Journal of Separation and Purification Technology* **188**(1): 399-422.

Khulood AA and Sara BJ 2010. Adsorption study for chromium on Iraqi Bentonite. *Journal of Baghdad Science* **7**(1):745-756.

Lund W 1994. The Pharmaceutical Codex, 12th The Pharmaceutical Press, London, pp.774-8512.

Mahboubeh H, Fatemeh Z, Zahra JR and Zohreh A 2014. Synthesis of cobalt ferrite (CoFe2O4) nanoparticles using combustion, coprecipitation, and precipitation methods: A comparison study of size, structural, and magnetic properties. *Journal of Magnetism and Magnetic Materials* **371**(1): 43-48.

Nasir RB, Nadagouda MN and Varma RS 2015. Magnetically retrievable catalysts for asymmetric synthesis. *Journal of Coordination Chemistry Reviews* **287**(1): 137-156.

Palak J, Manpreet K, Manmeet, K and Jaspreet, KG 2019. Comparative studies on spinal ferrite MFe2O4 (M = Mg/Co) nanoparticles as potential adsorbents for Pb(II) ions. *Journal of Bulletin of Materials Science* **77**(1): 1-9.

Paveena L, Vittaya A, Supapan S and Santi M 2011. Characterization and magnetic properties of nanocrystalline CuFe2O4, NiFe2O4, ZnFe2O4 powders prepared by the Aloe vera extract solution. *Journal of Current Applied Physics* **11** (1): 101-108.

Pehlivan E, Altun T and Parlayıcı S 2009. Utilization of barley straws as biosorbents for Cu^{2+} and Pb^{2+} ions. *Journal of Hazardous Materials* **164**(2): 982-986.

Roonasi P and Nezhad AY 2016. comparative study of a series of ferrite nanoparticles as heterogeneous catalysts for phenol removal at neutral pH. *Journal of Materials Chemistry and Physics* **172**(2): 143-149.

Salman GK, Bohan AJ and Jaed GM 2017. Use of Nano-Magnetic Material for Removal of Heavy Metals from Wastewater. *Journal of Engineering and Technology* **35**(9): 903-908.

Shaima'a JK and Ali AH 2018. The Effect of Catalyst Type on The Microstructure and Magnetic Properties of Synthesized Hard Cobalt Ferrite Nanoparticles. *Journal of University of Babylon, Engineering Science* **26**(4): 282-291.

Shen YF, Tang J, Nie ZH, Wang YD, Ren Y and Zuo L 2009. Preparation and application of magnetic Fe3O4 nanoparticles for wastewater purification. *Journal of Technology Separation and Purification Technology* **68**(2): 312-319.

Sivakumar M, Kanagesan S, Babu RS, Jesurani S and Velmurugan R 2012. Synthesis of CoFe2O4 powder via PVA assisted sol–gel process, *Journal of Materials Science: Materials in Electronics* **23**(5): 1045-1049.

Veena M and Robert HH 2002. The Role of F-400 granular activated carbon in scavenging dissolved copper ions from aqueous solution. *Journal of Energeia* **13**: 1-4.

Zhao D, Wu X, Guan H and Han E 2007. Study on supercritical hydrothermal synthesis of CoFe2O4 nanoparticles. *Journal of Supercritical Fluids* **42**(1): 226-233.

Received 10 September, 2021; Accepted 16 January, 2022